Effects of enhanced temperature and ultraviolet B radiation on a natural plankton community of the Beagle Channel (southern Argentina): a mesocosm study

S. Moreau, B. Mostajir, G. O. Almandoz, S. Demers, M. Hernando, K. Lemarchand, M. Lionard, B. Mercier, Sylvaine Roy, I. R. Schloss, et al.

Vol. 72: 155–173, 2014
doi: 10.3354/ame01694

AQUATIC MICROBIAL ECOLOGY
Aquat Microb Ecol

Published online May 7

Effects of enhanced temperature and ultraviolet B radiation on a natural plankton community of the Beagle Channel (southern Argentina): a mesocosm study

S. Moreau[1,2,*], B. Mostajir[3,4], G. O. Almandoz[5,6], S. Demers[2], M. Hernando[7], K. Lemarchand[2], M. Lionard[2,8], B. Mercier[2], S. Roy[2], I. R. Schloss[2,5,9], M. Thyssen[2,10], G. A. Ferreyra[2]

[1]Université catholique de Louvain (UCL), Louvain-la-Neuve 1348, Belgium

[2]Institut des Sciences de la Mer (ISMER), Université du Québec à Rimouski (UQAR), Rimouski, Québec G5L 3A1, Canada

[3]Laboratoire d'Ecologie des systèmes marins côtiers (ECOSYM), Université Montpellier 2-CNRS-IFREMER-IRD-Université Montpellier 1 (UMR 5119), 34095 Montpellier, France

[4]Centre d'écologie marine expérimentale MEDIMEER, Université Montpellier 2-CNRS (UMS 3301), 34200 Sète, France

[5]CONICET, C1033 AAV, Buenos Aires, Argentina

[6]División de Ficología, Facultad de Ciencias Naturales y Museo, Universidad Nacional de La Plata, B1900 FWA, La Plata, Argentina

[7]Comisión Nacional de Energía Atómica, Dpto. Radiobiología, B1650 KNA, San Martín, Argentina

[8]MERINOV, Centre d'Innovation de l'Aquaculture et des Pêches du Québec, Centre de la Côte-Nord, Direction de la production de la biomasse, Sept-Îles, Québec G4R 5B7, Canada

[9]Instituto Antártico Argentino, C1010 AAZ, Buenos Aires, Argentina

[10]Laboratoire d'Océanologie et de Géosciences UMR 8187, Maison de la Recherche en Environnements Naturels, 62930 Wimereux, France

ABSTRACT: Marine planktonic communities can be affected by increased temperatures associated with global climate change, as well as by increased ultraviolet B radiation (UVBR, 280–320 nm) through stratospheric ozone layer thinning. We studied individual and combined effects of increased temperature and UVBR on the plankton community of the Beagle Channel, southern Patagonia, Argentina. Eight 2 m^3 mesocosms were exposed to 4 treatments (with 2 replicates) during 10 d: (1) control (natural temperature and UVBR), (2) increased UVBR (simulating a 60% decrease in stratospheric ozone layer thickness), (3) increased temperature (+ 3°C), and (4) simultaneous increased temperature and UVBR (60% decrease in stratospheric ozone; + 3°C). Two distinct situations were observed with regard to phytoplankton biomass: bloom (Days 1–4) and post-bloom (Days 5–9). Significant decreases in micro-sized diatoms (>20 µm), bacteria, chlorophyll *a*, and particulate organic carbon concentrations were observed during the post-bloom in the enhanced temperature treatments relative to natural temperature, accompanied by significant increases in nanophytoplankton (10–20 µm, mainly prymnesiophytes). The decrease in micro-sized diatoms in the high temperature treatment may have been caused by a physiological effect of warming, although we do not have activity measurements to support this hypothesis. Prymnesiophytes benefited from micro-sized diatom reduction in their competition for resources. The bacterial decrease under warming may have been due to a change in the dissolved organic matter release caused by the observed change in phytoplankton composition. Overall, the rise in temperature affected the structure and total biomass of the communities, while no major effect of UVBR was observed on the plankton community.

KEY WORDS: Plankton · UVBR · Ozone hole · Increased temperature · Patagonia

*Corresponding author: s.moreau@uclouvain.be

INTRODUCTION

Warming due to increased greenhouse gas concentrations in the atmosphere, and increased ultraviolet B radiation (UVBR, 280–320 nm) through the thinning of the stratospheric ozone layer (Häder et al. 2007) at high latitudes of both hemispheres, are 2 of the main global processes with consequences for marine planktonic organisms. Strong regional warming has already triggered changes in Patagonia's water temperature (Thompson & Solomon 2002), and further warming is expected in the next few decades (Houghton et al. 2001). Indeed, models predict an increase of 1.7 to 3.9°C (median of 2.5°C) of the annual temperature in the southern part of South America by 2080–2099 (Christensen et al. 2007 [IPCC 2007]). Increasing water temperature may have both positive and negative effects on marine microbial communities. In this sense, the increase in metabolic activity (e.g. primary production; Ingram 1979) might be considered a positive effect. In contrast, stenothermal species may not be able to tolerate high water temperatures (e.g. Williamson et al. 2002). In Patagonia, Giordanino et al. (2011) observed that among 4 species of cyanobacteria, only 2 benefited from a 5°C increase in water temperature, in terms of photosynthetic performance. An increase in water temperature may also have a more general effect on the whole microbial community, possibly favoring small cells (i.e. pico- and nanophytoplankton) over larger cells (i.e. microphytoplankton) as shown by Morán et al. (2010) for the North Atlantic Ocean, by Montes-Hugo et al. (2009) for the western Antarctic Peninsula, and by Li et al. (2009) in the Arctic Ocean as a result of regional warming and Arctic waters freshening.

The thinning of the stratospheric ozone layer (i.e. the so-called 'ozone hole') has been mostly documented over the Antarctic (McKenzie et al. 2007) but is also a threat to other regions of the world such as Patagonia and the Arctic (Manney et al. 2011). Through the rotation of the polar vortex, Patagonia is periodically exposed to the ozone hole and therefore to high UVBR (Orce & Helbling 1997, Casiccia et al. 2008). In fact, Patagonia has been exposed to the ozone hole since at least 1990 (Díaz et al. 2006). Under the Antarctic ozone hole, a 60% decrease in the stratospheric ozone layer thickness is commonly observed and leads to a 510% increase in UVBR (Booth & Madronich 1994). Because the stratospheric ozone layer is not expected to fully recover before 2070 (McKenzie et al. 2007), it will remain a threat to marine organisms for the next few (3–4) decades. UVBR may have strong deleterious effects on marine organisms such as phytoplankton, bacteria, and microzooplankton which compose the microbial communities (for a review of potential UVBR effects see: Sinha & Häder 2002, Häder & Sinha 2005, Häder et al. 2007, Llabrés et al. 2012, Ruiz-González et al. 2013). In addition to the negative effects of UVBR at the organism level, there may be UVBR effects on the whole microbial community through trophic interactions (e.g. Mostajir et al. 1999a, Ferreyra et al. 2006).

Increases in water temperature and in UVBR may affect the microbial community separately, synergistically, or antagonistically. For example, increased temperatures may counter the negative effects of UVBR by increasing metabolic activities and, therefore, by increasing the rates of enzymatic photorepair mechanisms (Bouchard et al. 2006). Halac et al. (2010) observed lower UVBR-induced photoinhibition in 2 diatom species when they were exposed to a 5°C increase in water temperature. In contrast, an increase in water temperature may increase the stratification of the water column (Sarmiento et al. 2004), which may in turn confine microorganisms within a shallow water column and maximize their exposure to UVBR as observed by Moreau et al. (2010) in early spring in the western Antarctic Peninsula. Few studies have investigated the combined effects of temperature and UVBR on aquatic microbial communities. Rae & Vincent (1998) observed no synergistic effects of temperature and UVBR on subarctic freshwater communities. Fouilland et al. (2013) observed both a decrease in bacterial production and an increase in primary production under warming in Mediterranean coastal waters. Working on the same experiment, Vidussi et al. (2011) observed significant shifts in the plankton food web structure and function under warming. However, the effects of UVBR on the microbial community were rarely significant during their experiment. Finally, Lionard et al. (2012) reported a positive effect of a 3°C temperature increase on the abundance of diatoms in the St. Lawrence Estuary but low effects of UVBR.

With our current level of knowledge, it is not possible to accurately predict the outcome of the combined increase in water temperature and UVBR which threatens Patagonia because of trophic interactions and the physical and optical dynamics of the marine environment. The microbial community is at the base of the marine food web and plays a crucial role in marine ecosystems. Its structure, from the microbial loop to the herbivorous food web (Legendre & Rassoulzadegan 1995), will determine the fate and allocation of carbon within the planktonic food web,

as well as the transfer of carbon towards higher trophic level predators and export (Legendre & Rivkin 2002). In addition, its structure has an impact on the role of the marine community in terms of CO_2 dynamics (i.e. the biological pump) as shown by Schloss et al. (2007) and Moreau et al. (2012, 2013). There is therefore a great need to consider the whole microbial community when studying the combined effects of increases in water temperature and UVBR. In this context, the goal of this study was to test for single and combined effects of increased temperature and UVBR on the planktonic community of the Beagle Channel in Southern Patagonia using a mesocosm approach.

MATERIALS AND METHODS

Experimental set up

The experiment was conducted in Ushuaia, Tierra del Fuego Province (54° 49′ S, 68° 19′ W, Southern Patagonia, Argentina, Fig. 1), during the summer 2008: from 10 February (Day 0), to 19 February (Day 9). The mesocosms were filled with sub-surface (~5 m depth) water from the Beagle Channel, a sub-Antarctic coastal marine environment that connects the Atlantic and Pacific oceans. Experiments were run in 8 stainless steel land-based mesocosms (2 m^3, 1.7 m deep and 1.2 m diameter) that were set up for the present experiment.

Fig. 1. Location (star) of the mesocosm setup in Ushuaia, Tierra del Fuego (Patagonia), Argentina

Four treatments were applied in duplicate: (1) natural temperature and natural UVBR ('control'), (2) high temperature (+3°C) and natural UVBR ('high temperature'), (3) natural temperature and high UVBR (simulating a 60% decrease in stratospheric ozone layer thickness; 'high UVBR'; Díaz et al. 2006), and (4) simultaneous high temperature and high UVBR (simulating a 60% decrease in stratospheric ozone layer thickness and +3°C; 'high temperature+UVBR'). The treatments were chosen to mimic the worst, but realistic, conditions for, respectively, the presence of the ozone hole above Patagonia and the increase in temperature expected by 2100 (Christensen et al. 2007 [IPCC 2007]).

All mesocosms were exposed to the natural incident irradiance except for the high UVBR and high temperature+UVBR treatments, in which natural irradiance was supplemented with UVBR lamps. For these 2 treatments, a set of 4 UVB lamps (UVB fluorescent tubes, Philips TL40W-12RS) was fixed at 20 cm above the surface of each mesocosm. A set of 4 dummy lamps was added to the other mesocosms in order to obtain similar shading conditions for all treatments. In addition, ultraviolet C radiation (UVCR, <280 nm) was removed by wrapping the UVB tubes with acetate films (SABIC polymer shapes, cat. Nr. 70600605; Díaz et al. 2006). The films were changed every day because of the potential acetate degradation. The UVB lamps were switched on for 5 h (11:45 to 17:45 h) centered at local noon (~15:15 h) from 12 February (Day 2) to 19 February (Day 9). During the experiment, incident irradiance (photosynthetically active radiation, PAR, 400–700 nm; ultraviolet A radiation, UVAR, 320–400 nm, and UVBR) was monitored at 15 min intervals using a ground radiometer (GUV-541; Biospherical Instruments). The wavelengths considered were 305 and 313 nm (UVBR); 320, 340, and 380 nm (UVAR), and 400–700 nm in the PAR range. In addition, irradiance profiles within the mesocosms at the selected wavelengths (i.e. 305, 313, 320, 340, 380, and 400–700 nm) for the UVBR, UVAR, and PAR were obtained every day at local noon (~15:15 h) with a profiling radiometer (PUV-542T; Biospherical Instruments). After each profile, the PUV was rinsed first with nanopure water and subsequently with seawater from the next mesocosm to be sampled, to avoid contamination among the experi-

mental units. A 3°C increase in temperature (2100 trend, Christensen et al. 2007 [IPCC 2007]) was applied to the high temperature and high temperature+UVBR treatments 1 d before the experiment, and temperature in the mesocosms was then maintained constant from 10 February (Day 0) to 19 February (Day 9). Temperature in the mesocosms was controlled using a N480D electronic controller placed 1 m below the water surface, and data were recorded every 60 s. The mesocosm temperature was changed or maintained with external heat exchangers made of fiberglass outside and of a series of stainless steel tubes inside. These external heat exchangers allowed heat exchanges between mesocosm water and an alternate warm–cool external water source as described by Thyssen et al. (2011).

Before filling the mesocosms with seawater, they were rinsed successively with a chlorinated solution and fresh water. On Day 0, the mesocosms were filled with seawater from the Beagle Channel filtered through a 300 µm Nitex net to exclude large zooplankton. Seawater was poured into a single container that distributed seawater homogenously among the 8 mesocosms. The container was previously rinsed with a chlorinated solution and with fresh water. To initiate a phytoplankton bloom, a 1 l solution of 8.088 g KNO_3, 0.6805 g KH_2PO_4 and a 20.35 ml solution of 30 g l^{-1} $NaSiO_3$ was prepared and 0.125 ml of this solution was added to each mesocosm (on Day 1) to increase nitrogen, phosphorus, and silicium concentrations by 5, 0.31 and 0.39 µM, respectively. Seawater within the mesocosms was continuously mixed from the bottom to the surface with a pump at a turnover rate of 1000 l h^{-1}. To ensure that mixing was performed correctly, vertical profiles of water column properties (pH, dissolved oxygen, temperature, and salinity; data not shown) were measured 3 times a day with a U-10 HORIBA multiparameter probe. These profiles confirmed the homogeneity of the water column. At night, the mesocosm openings were sealed with plastic covers to avoid external contamination. One of the control mesocosms presented technical difficulties and the results are not presented here.

Sampling and sample analyses

Unless specified otherwise, all water samples were collected through water outlets, located at the bottom of the mesocosms, every day at 17:45 h after the lamp increased UVBR exposure. Because of the continuous mixing of the mesocosms, water samples were considered as representative of the whole water column. For the analysis of pigment concentrations by high performance liquid chromatography (HPLC), 400 to 600 ml of mesocosm water were filtered onto 25 mm diameter Whatman GF/F glass fiber filters once or twice a day (8:00 and 17:45 h). Filters were wrapped in aluminum foil, frozen in liquid nitrogen, and stored at −80°C until analysis within 1 mo after the end of the experiment. Concentrations of major phytoplankton pigments were determined using a Thermo Fisher HPLC system following the method of Zapata et al. (2000). The relative contribution of major algal groups to total chlorophyll *a* (chl *a*) was estimated using the CHEMTAX 195 program developed by Mackey et al. (1996). The initial matrix of accessory pigments to chl *a* ratios is presented in Table 1 and includes algal groups identified by microscopy during this study as well as pigment-based types of phytoplankton from Jeffrey & Wright (2006).

For the analyses of nutrients (nitrate plus nitrite and phosphate), 2 replicate 60 ml samples were taken in each mesocosm every day at 08:00 h. Samples were filtered onto precombusted Whatman GF/F filters and kept frozen at −20°C until analysis within a month after the end of the experiment. The analysis of nutrients was performed using a Bran Luebbe Auto Analyzer 3 system following the method of Grasshof et al. (1983).

For the analysis of the particulate organic carbon and nitrogen concentrations (POC and PON, respectively), duplicate 1 to 2 l samples were filtered onto pre-combusted GF/F filters and stored at −20°C until analysis with a CHN elemental analyzer (Costech 4010) within 1 mo after the end of the experiment.

For flow cytometry, water aliquots were put into 4.5 ml cryovials, fixed with glutaraldehyde (final concentration 0.2%) and kept frozen at −80°C until analysis within 1 mo after the end of the experiment. Samples were analyzed for phytoplankton and bacterial abundances using an EPICS® ALTRA™ flow cytometer (Beckman Coulter®) according to Moreau et al. (2010). Picophytoplankton (<2 µm), small nanophytoplankton (2–10 µm), and large nanophytoplankton (10–20 µm) were discriminated. Bacteria with high and low nucleic acid content (HNA and LNA subgroups, respectively) were discriminated (Lebaron et al. 2001). Total free bacterial abundance was used to describe the bacterial community distribution, and the proportion of HNA cells (%HNA) was calculated to determine the importance of the HNA and LNA sub-populations in the whole community (Gasol et al. 1999, Gasol & Giorgio 2000, Vaqué et al.

2001). The carbon content of microorganisms was calculated using different conversion factors for the different size classes: 220 fg C µm^{-3} for nanophytoplankton (Tarran et al. 2006), 1.5 pg C cell^{-1} for picophytoplankton, and 12 fg C cell^{-1} for bacteria (Zubkov et al. 2000a,b).

Samples for the identification and enumeration of phytoplankton and microzooplankton were fixed in Lugol's solution at 2% final v/v concentrations in 300 ml glass amber bottles and kept at 4°C. Organisms were identified to the lowest possible taxonomic level and enumerated for Days 1 to 8 (phytoplankton) and for Days 2, 4, 6, and 8 (microzooplankton), using an inverted microscope according to the procedures described by Utermöhl (1958). Microphytoplankton included all chain-forming diatoms (e.g. *Chaetoceros* spp., *Skeletonema* spp., *Pseudo-nitzschia* spp.) and those single cells >20 µm. Cell biovolumes were calculated using the geometric shapes proposed by Hillebrand et al. (1999) and corrected to account for cell shrinkage caused by fixation of samples (Montagnes et al. 1994). Cell carbon content was calculated with 2 different C to volume (V) ratios depending on algal groups: pg C cell^{-1} = 0.288 V$^{0.811}$ for diatoms and pg C cell^{-1} = 0.216 V$^{0.939}$ for all other algal groups (Menden-Deuer & Lessard 2000). Cell carbon content of microzooplankton was calculated from the C:V ratio of Putt & Stoecker (1989), where C:V = 0.19 pg µm^{-3} for ciliates and using the carbon conversion factor of 220 fg C µm^{-3} for heterotrophic flagellates (Børsheim & Bratbak 1987). It is worth noting that the fixation of samples with Lugol's solution may cause an underestimation of coccolithophorids in microscopy. However, as described below, the tendencies in the abundance of prymnesiophytes observed under the microscope were additionally confirmed by other techniques such as flow cytometry and HPLC.

To test the significance of the observed differences between treatments, repeated measures ANOVA tests were run. If differences between treatments were found, post-hoc Tukey tests were performed. If normality and/or homoscedasticity were not verified, data were normalized with a ranked transformation (i.e. chl *a*, %HNA, pico- and nanophytoplankon). For these variables, Friedman repeated measures ANOVA tests on ranks were run. The daily doses of UVBR and UVAR were calculated from

Table 1. CHEMTAX initial and final pigment matrix ratios for major algal groups present in the Beagle Channel, Ushuaia, Argentina. The various types of phytoplankton were taken from Jeffrey & Wright (2006). Chl: chlorophyll; Mg-DVP: Mg-2,4-divinyl pheoporphyrin a_5 monomethyl ester; Perid: peridinin; Uriol: uriolide; BFU: 19'-butanoyloxyfucoxanthin; Fuco: fucoxanthin; Neo: neoxanthin; Pras: prasinoxanthin; Viola: violaxanthin; HFU: 19'-hexanoyloxyfucoxanthin; DDX: sum of diadinoxanthin and diatoxanthin; Zea: zeaxanthin; Lut: lutein; Croco: crocoxanthin; εε-car: ε,ε-carotene; ββ-car: β,β-carotene

Initial matrix	Chl c_1	Chl c_2	Chl c_3	Mg-DVP	Perid	Uriol	BFU	Fuco	Neo	Pras	Viola	HFU	DDX	Zea	Lut	Croco	Chl *b*	εε-car	ββ-car
Chlorophytes	0	0	0	0	0	0	0	0	0.040	0	0.040	0	0	0.006	0.137	0	0.184	0.001	0.222
Diatoms	0.043	0.057	0	0	0	0	0	0.490	0	0	0	0	0.106	0	0	0	0	0	0.017
Euglenophytes	0	0	0	0	0	0	0	0	0.016	0	0	0	0.283	0	0	0	0.360	0	0.019
Prasinophytes (Type3)	0	0	0	0.023	0	0.011	0	0	0.062	0.121	0.026	0	0	0.049	0.004	0	0.406	0	0
Cryptophytes	0	0.064	0	0	0	0	0	0	0	0	0	0	0	0	0	0.185	0	0.020	0
Prymnesiophytes (Type 8)	0	0.020	0.151	0	0	0	0.011	0.261	0	0	0	0.220	0.099	0	0	0	0	0	0.010
Dinophytes (Type 1)	0	0.221	0	0	0.498	0	0	0	0	0	0	0	0.186	0	0	0	0	0	0
Chrysophytes (Type 1)	0	0.080	0	0	0	0	0	0.349	0	0	0.047	0	0	0	0	0	0	0	0.015
Final matrix	Chl c_1	Chl c_2	Chl c_3	Mg-DVP	Perid	Uriol	BFU	Fuco	Neo	Pras	Viola	HFU	DDX	Zea	Lut	Croco	Chl *b*	εε-car	ββ-car
Chlorophytes	0	0	0	0	0	0	0	0	0.028	0	0.022	0	0	0.004	0.079	0	0.097	0.001	0.142
Diatoms	0.032	0.063	0	0	0	0	0	0.319	0	0	0	0	0.025	0	0	0	0	0	0.009
Euglenophytes	0	0	0	0	0	0	0	0	0.008	0	0	0	0.165	0	0	0	0.233	0	0.010
Prasinophytes (Type3)	0	0	0	0.011	0	0.005	0	0	0.032	0.077	0.016	0	0	0.025	0.002	0	0.267	0	0
Cryptophytes	0	0.058	0	0	0	0	0	0	0	0	0	0	0	0	0	0.162	0	0.015	0
Prymnesiophytes (Type 8)	0	0.010	0.074	0	0	0	0.005	0.112	0	0	0	0.240	0.050	0	0	0	0	0	0.005
Dinophytes (Type 1)	0	0.091	0	0	0.264	0	0	0	0	0	0	0	0.118	0	0	0	0	0	0
Chrysophytes (Type 1)	0	0.058	0	0	0	0	0	0.208	0	0	0.032	0	0	0	0	0	0	0	0.012

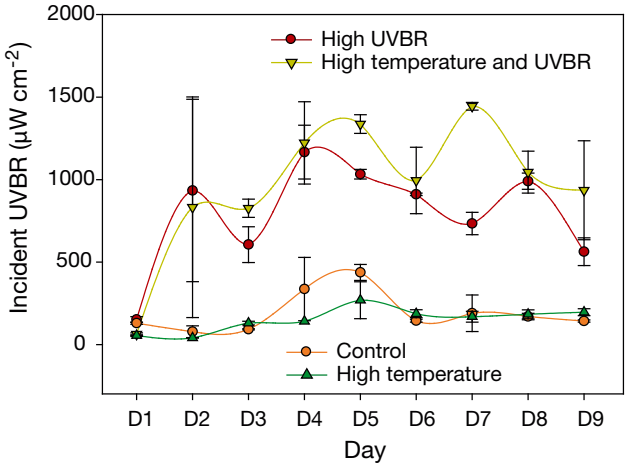

Fig. 2. Incident ultraviolet B radiation (average ± SD UVBR, µW cm^{-2}) at the surface of the experimental mesocosms. The 4 treatments were as follows: (1) control: natural temperature and natural UVBR; (2) high temperature: high temperature (+3°C) and natural UVBR; (3) high UVBR: natural temperature and high UVBR (simulating a 60% decrease in stratospheric ozone layer thickness); and (4) high temperature+UVBR: simultaneous high temperature and high UVBR

Orce & Helbling (1997) as: UVBR = 59.5 × E_{305} + 4.1 × E_{320} and UVAR = 87.4 × E_{340} − 2.4 × E_{380}, with E_{305}, E_{320}, E_{340}, and E_{380} the incident irradiance at 305, 320, 340, and 380 nm, respectively. For the analysis of optical data, the depth of penetration of 10% of the incident light was calculated from the Beer's-Lambert law as $Z_{10\%}$ = 2.3/$K_d(\lambda)$ (Kirk 1994). The $Z_{10\%}$ depth was used as the limit of the photoactive layer (i.e. the depth at which the effects of UVBR cease; Neale et al. 2003). Finally, the mean irradiance from the surface of the mesocosm to the depth of penetration of 10% of the incident light ($Z_{10\%}$) was calculated as in Vasseur et al. (2003). Average ± SD are reported throughout.

RESULTS

Irradiance, temperature, chl *a*, and nutrient, PON, and POC concentrations

The daily natural dose of UVBR, UVAR, and PAR averaged 50.3 ± 11.8, 796.3 ± 130.6, and 7587.3 ± 1767.4 kJ m^{-2} d^{-1}. The stratospheric ozone layer thickness averaged 281.8 ± 17.7 Dobson Units (DU), with a minimum of 255 DU. In addition, the UVBR:UVAR ratio was significantly correlated to the thickness of the stratospheric ozone (r^2 = 0.699, $p < 0.01$). Within 2 h before and after local noon (~15:15 h), the incident UVBR at the surface of the normal UVBR mesocosms averaged 171.9 ± 105.47 µW cm^{-2} s^{-1}. At the surface of the increased UVBR mesocosms, the incident UVBR around local noon averaged 877.4 ± 394.3 µW cm^{-2} s^{-1} and corresponded to 510.2% of the UVBR irradiance in the normal UVBR treatments (Fig. 2). Moreover, the mean UVBR irradiance at 305 nm from the surface of the mesocosm to the depth of penetration of 10% of the incident light ($Z_{10\%}$) was 5 ± 0.8 µW cm^{-2} for the high UVBR treatments and 0.8 ± 0.4 µW cm^{-2} for the normal UVBR treatments. The mean UVBR irradiance at 305 nm from the surface to $Z_{10\%}$ was significantly higher in the high UVBR treatments from Day 2 to Day 9 ($p < 0.01$) relative to the normal UVBR treatments. In contrast, no significant differences were observed in the diffuse attenuation coefficient between the increased and normal UVBR treatments at 305 nm, with K_d of 3.29 ± 0.3 m^{-1} for the increased UVBR treatments and K_d of 3.45 ± 0.97 m^{-1} for the normal UVBR treatments. Because no differences in K_d were observed between treatments, no significant differences in the $Z_{10\%}$ depths were observed between the normal and high UVBR treatments at 305 nm. The water temperature inside the low temperature treatments was, on average, 12.05 ± 0.26°C from Day 1 to Day 9 of the experiment. In the elevated temperature treatments, water temperature was, on average, 14.92 ± 0.18°C from Day 1 to Day 9.

Chl *a* was low at the beginning of the experiment and showed no difference between treatments, with an average chl *a* of 1.6 ± 0.12 µg l^{-1} on Day 0 (Fig. 3a). Following the addition of nutrients in the mesocosms, chl *a* increased regularly from Day 1 to Day 4 when it reached a maximum of 9.8 ± 0.7 µg l^{-1}, averaged among all mesocosms. The increase in chl *a* was considered as the bloom phase between Days 0 and 4. During the post-bloom phase from Days 5 to 9, chl *a* declined in all mesocosms, although this decrease was significantly faster in the high temperature treatments with significant differences between the high and low temperature treatments on Days 5, 6, and 7 (Fig. 3, $p < 0.01$). On Day 9, chl *a* had decreased in all mesocosms to an average final value of 4.2 ± 0.3 µg l^{-1}.

Initial nitrite plus nitrate and phosphate concentrations were 2.7 ± 1.5 and 0.5 ± 0.1 µM, respectively (Fig. 3b,c). Nutrients were added to the mesocosms on Day 1, and concentrations on Day 2 were 7.8 ± 0.6 and 0.8 ± 0.04 µM for nitrite plus nitrate and phosphate, respectively. After Day 2, and along with the observed increase in chl *a*, both nitrite and nitrate and phosphate decreased regularly to reach minimal concentrations of 0.9 ± 0.2 and 0.3 ± 0.06 µM on Day 5, respectively. Throughout the whole experiment, there were no significant differences in nutrient concentrations among the 4 treatments.

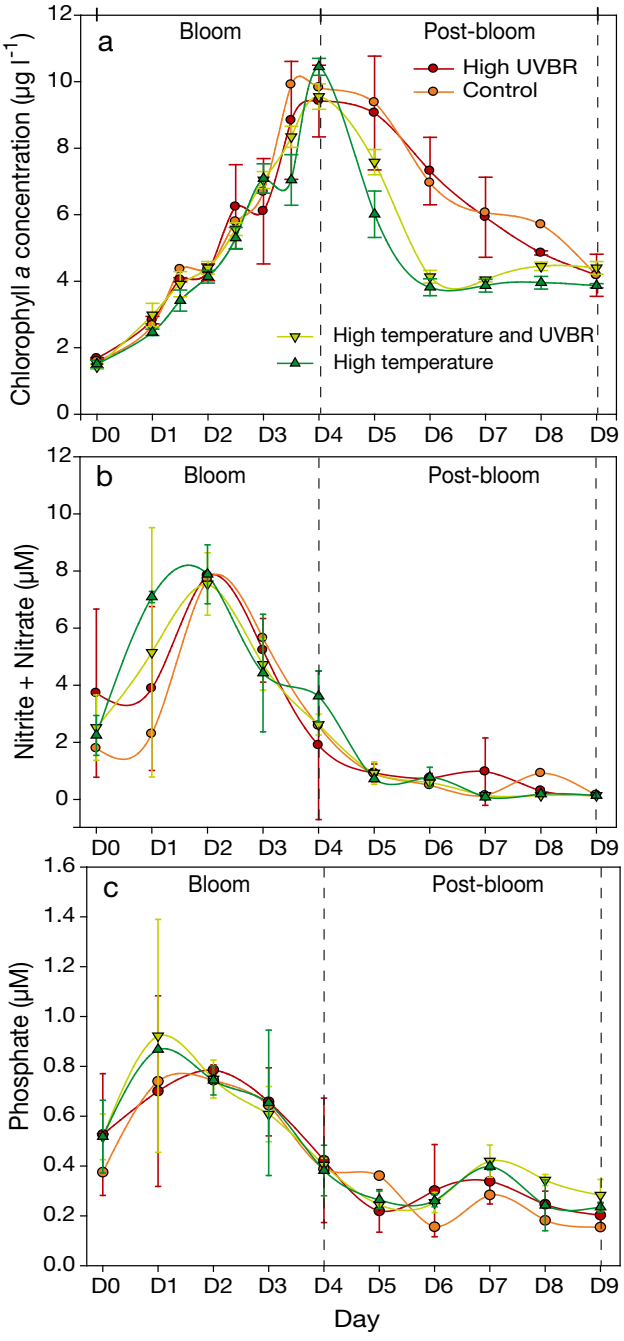

Fig. 3. Average (± SD) (a) chl *a* concentration (µg l^{-1}), (b) nitrite and nitrate concentration (µM), and (c) phosphate concentration (µM) in the experimental mesocosms (see Fig. 2 for descriptions of the 4 treatment groups)

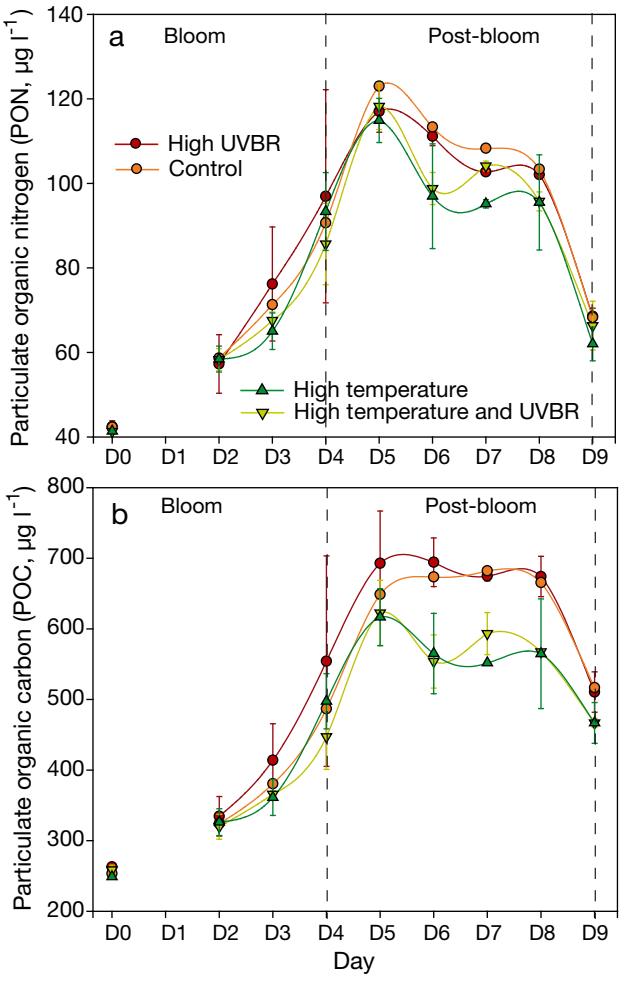

Fig. 4. Average (± SD) (a) particulate organic nitrogen (PON) concentration (µg l^{-1}) and (b) particulate organic carbon (POC) concentration (µg l^{-1}) in the experimental mesocosms (see Fig. 2 for descriptions of the 4 treatment groups)

Both PON and POC concentrations increased during the bloom phase from initial concentrations of 41.9 ± 0.8 and 257.1 ± 6.7 µg l^{-1}, respectively, to maximal concentrations of 113.1 ± 13.3 and 618.1 ± 89.3 µg l^{-1} reached on Day 5, 1 d after the chl *a* maximum (Fig. 4a,b). After reaching these maximal concentrations, PON decreased regularly during the post-bloom phase, while POC concentrations stayed high from Day 5 to Day 8 before they also decreased on Day 9. There were no differences in the accumulation of PON between the treatments. In contrast, POC concentrations were markedly lower in the high temperature treatments during the post-bloom, showing a similar trend to chl *a* (Fig. 4b). However, this difference was only significant on Day 6 ($p < 0.05$).

Structure and dynamics of phytoplankton

Fig. 5a–c shows abundances of picophytoplankton (<2 µm) and small (2–10 µm) and large (10–20 µm) nanophytoplankton throughout the experiment. Picophytoplankton bloomed very early in the experiment, increasing in abundance from average initial con-

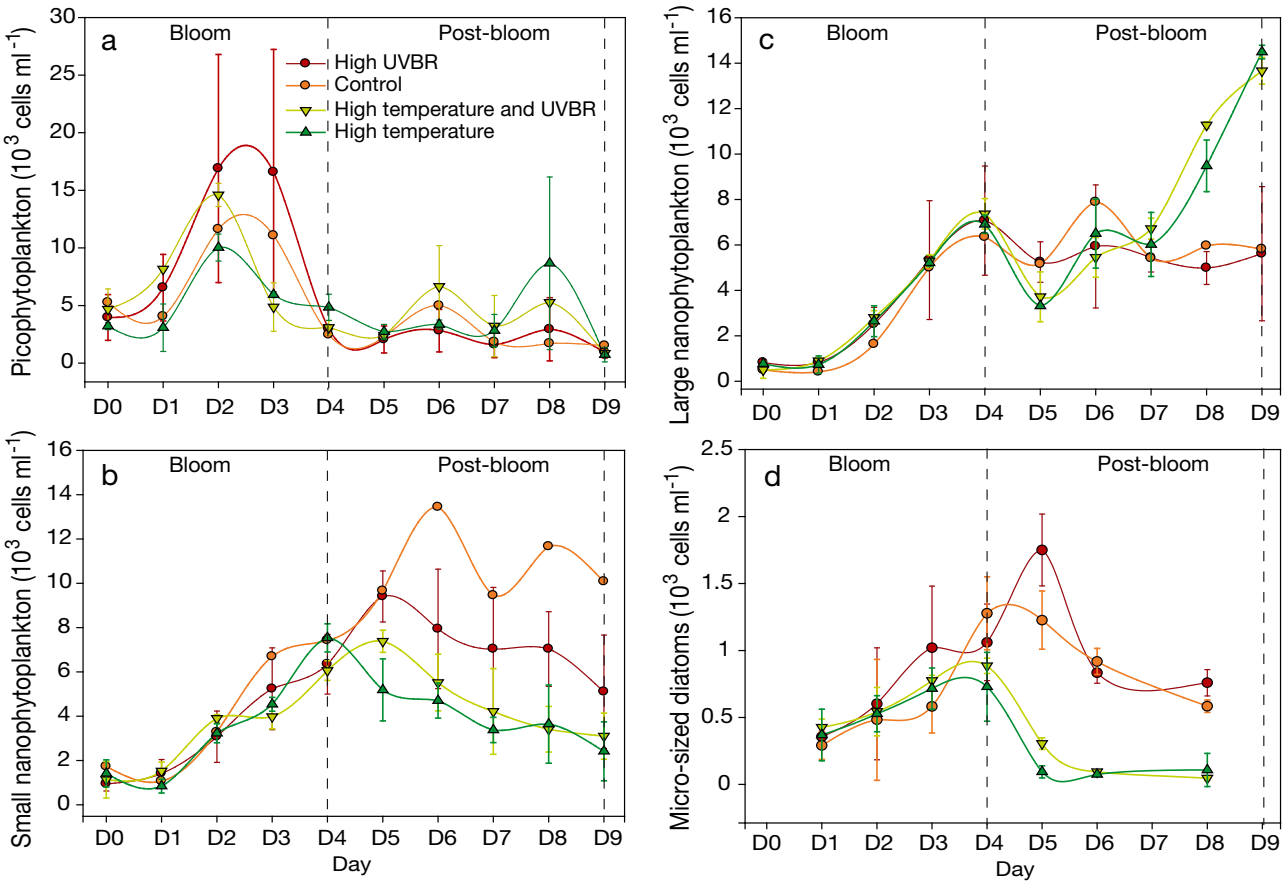

Fig. 5. Average (± SD) (a) picophytoplankton abundance (cells ml^{-1}), (b) small (2–10 µm) nanophytoplankton abundance (cells ml^{-1}), (c) large (10–20 µm) nanophytoplankton abundance (cells ml^{-1}), and (d) micro-sized (>20 µm) diatom abundance (cells ml^{-1}) in the experimental mesocosms (see Fig. 2 for descriptions of the 4 treatment groups)

centrations of 4.1 ± 1.3 × 10^3 cells ml^{-1} on Day 0 to maximal concentrations of 13.5 ± 5.1 × 10^3 cells ml^{-1} on Day 2 (Fig. 5a). After Day 4 and to the end of the experiment, picophytoplankton abundance stayed low (with an average abundance of 3.1 ± 2.5 × 10^3 cells ml^{-1}). There were no significant differences in the abundance of picophytoplankton between treatments.

Small nanophytoplankton was mainly composed of coccolithophorids resembling *Emiliania huxleyi* and other prymnesiophytes, of prasinophytes (*Pyramimonas*-like), of cryptophytes, and of other unidentified flagellates. The initial abundance of small nanophytoplankton on Day 0 was 1.25 ± 0.05 × 10^3 cells ml^{-1} on average. Their abundance then increased in all treatments up to Day 5, when it reached an average concentration of 7.7 ± 2.1 × 10^3 cells ml^{-1} (Fig. 5b). After Day 5, small nanophytoplankton decreased to the end of the experiment in all the treatments except for the control treatment, in which it kept increasing. Overall, the abundance of small nanophytoplankton was lower in the high temperature treatments compared to the normal temperature treatments during the post-bloom, although that difference was not significant ($p > 0.05$).

Large nanophytoplankton was mainly composed of small diatoms of the genus *Thalassiosira* and undetermined prymnesiophytes. Their initial abundance was 0.67 ± 0.02 × 10^3 cells ml^{-1} on average and increased up to Day 4, reaching an average concentration of 7 ± 1.1 × 10^3 cells ml^{-1} (Fig. 5c). After Day 4, their abundance followed a plateau-like phase in all treatments. For the last 2 d of the experiment, their abundance was significantly higher ($p < 0.05$ and $p < 0.01$ for Days 8 and 9, respectively) in the high temperature (with an average abundance of 12.2 ± 2.1 × 10^3 cells ml^{-1}) than in the low temperature treatments (with an average abundance of 5.5 ± 1.4 × 10^3 cells ml^{-1}). This increase in large nanophytoplankton abundance was linked to the gradual replacement of diatoms by prymnesiophytes in the high temperature treatments (see below). Neither the pico- nor the nanophytoplankton followed the evolution of chl *a* illustrated in Fig. 3a.

Microphytoplankton was mainly composed of diatoms; dinoflagellates contributed to less than 1% of the total microphytoplankton carbon biomass (data not shown). Diatoms, which contributed to ~98% of the microphytoplankton carbon biomass, were composed of 2 main taxa, viz. *Thalassiosira* spp. (average diameter 25 µm) and *Asterionellopsis glacialis*, with an average contribution of 64.1 and 8.2% of the total microphytoplankton carbon biomass, respectively. The abundance of micro-sized diatoms throughout the experiment is presented in Fig. 5d. The abundance of micro-sized diatoms increased from the beginning of the experiment up to Day 4, after which it started to decrease with a trend similar to that of chl *a* (Fig. 3a). During the post-bloom phase of the experiment, there was a significant difference in the abundance of micro-sized diatoms between the natural and high temperature treatments (i.e. on Days 5, 6, and 8; $p < 0.01$), which is also similar to the observed chl *a* trend and consistent with the CHEMTAX results presented below.

HPLC pigment and CHEMTAX analyses are consistent with the above results, with diatoms largely dominating phytoplankton biomass in all treatments from Day 0 to Day 4 with ca. 50% of the phytoplankton biomass (Fig. 6). Euglenophytes and prasinophytes were the second and third groups, representing 10 to 25% of the biomass at the beginning of the

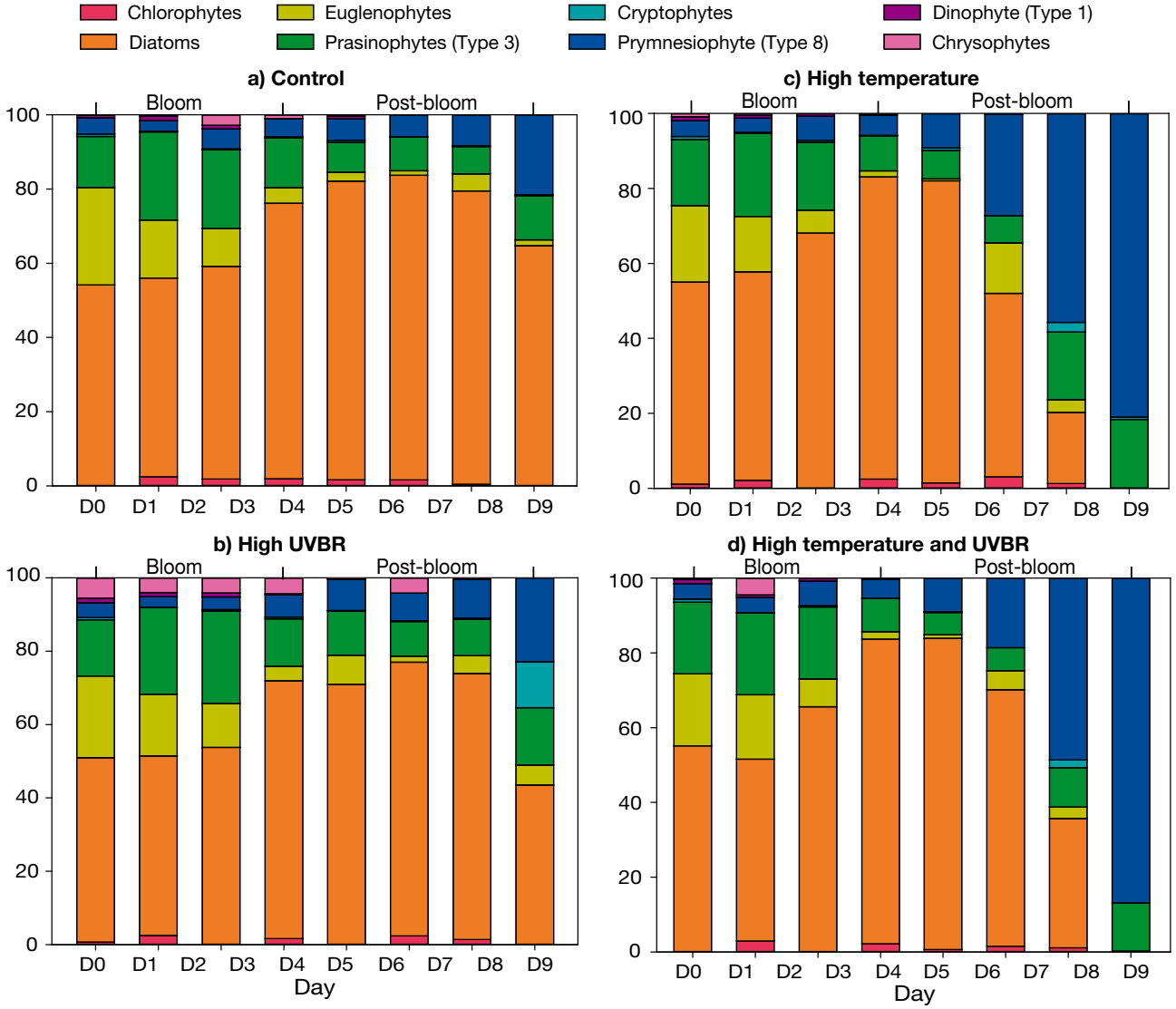

Fig. 6. Phytoplankton community groups, expressed as a percentage of the total chl *a* concentration (µg chl *a* l^{-1}), obtained from CHEMTAX analysis for the (a) control, (b) high UVB, (c) high temperature, and (d) high temperature+UVBR treatments (see Fig. 2 for descriptions of the 4 treatment groups). Pigment-based types of phytoplankton were assessed from Jeffrey & Wright (2006)

experiment. Over the course of the experiment, however, euglenophytes progressively disappeared in all treatments while prasinophytes remained stable. On Day 0, prymnesiophytes only represented ca. 4% of the biomass. An increase in prymnesiophyte pigment biomass was observed during the chlorophyll post-bloom phase. This increase was slight in mesocosms at normal temperature, with prymnesiophytes representing ~20% of the pigment biomass (Fig. 6a,b). However, this chlorophyll post-bloom increase was larger in the high temperature treatments (Fig. 6c,d), and prymnesiophytes progressively replaced diatoms and dominated the phytoplankton biomass with ca. 80% of the biomass on Day 7.

Dynamics of bacteria

The average bacterial abundance was 2.09 ± 0.15 × 10^6 cells ml^{-1} on Day 0, then it regularly decreased in all mesocosms to an average abundance of 1.17 ± 0.12 × 10^6 cells ml^{-1} on Day 3 (Fig. 7a). From Day 3 up to Day 7, the bacterial abundances increased in all mesocosms to an average of 2.56 ± 0.33 × 10^6 cells ml^{-1}. After this, bacterial abundance kept increasing in the normal temperature treatments to a maximum abundance of 3.06 ± 0.17 × 10^6 cells ml^{-1} on Day 9, while it decreased in the high temperature treatments to a final abundance of 1.83 ± 0.18 × 10^6 cells ml^{-1} on Day 9. Clear and significant differences were observed between the normal and high temperature treatments on Days 8 and 9 ($p < 0.01$).

In all mesocosms, %HNA was relatively low at the beginning of the experiment (with an average of 50.2 ± 1.1%; Fig. 7b). %HNA stayed low until Day 3, after which it increased regularly in all mesocosms to reach a maximum of 71.5 ± 2.4% on Day 8. This increase was consistent with the increase in bacterial abundance observed during the experiment. Interestingly, %HNA decreased slightly towards the end of the experiment on Day 9 following the observed decrease in bacterial abundance (Fig. 7a,b). Throughout the experiment, %HNA was significantly higher in the high temperature treatments only on Days 3 and 4 ($p < 0.01$).

Dynamics of heterotrophic flagellates and ciliates

Microzooplankton biomass consisted mainly of 1 species of heterotrophic flagellate (*Ebria tripartita*, 20–30 µm), and of small (<20 µm) and large (>20 µm) unidentifiable ciliates. They contributed to 9, 24, and

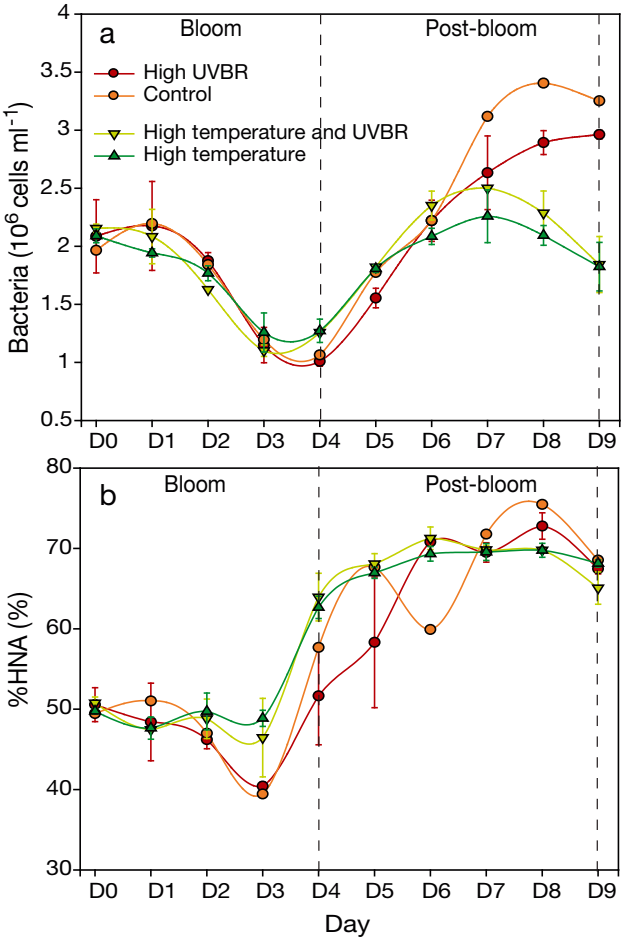

Fig. 7. Average (± SD) (a) bacterial abundance (cells ml^{-1}) and (b) percent of high nucleic acid content bacteria (HNA, %) in the experimental mesocosms (see Fig. 2 for descriptions of the 4 treatment groups)

66%, respectively, of the microzooplankton carbon biomass. This represents a rather small contribution of heterotrophic flagellates to the total microzooplankton biomass and abundance. This could have been due to conservation problems or difficulties in the counting of heterotrophic flagellates, and more particularly with the small (<20 µm) heterotrophic flagellates which may have been confused with other small autotrophic flagellates. Hence, small heterotrophic flagellates may have been present in greater numbers than reported here.

Except in the high UVBR treatment, total microzooplankton abundance increased from Day 2 to Day 6 to an average abundance of 133.8 ± 98 cells ml^{-1} on Day 6 and decreased between Days 6 and 8 to an average final abundance of 27.5 ± 15.6 cells ml^{-1} (Fig. 8a). The abundance of the small ciliates followed the same pattern, increasing from the beginning of the experiment to Day 6 before decreasing to

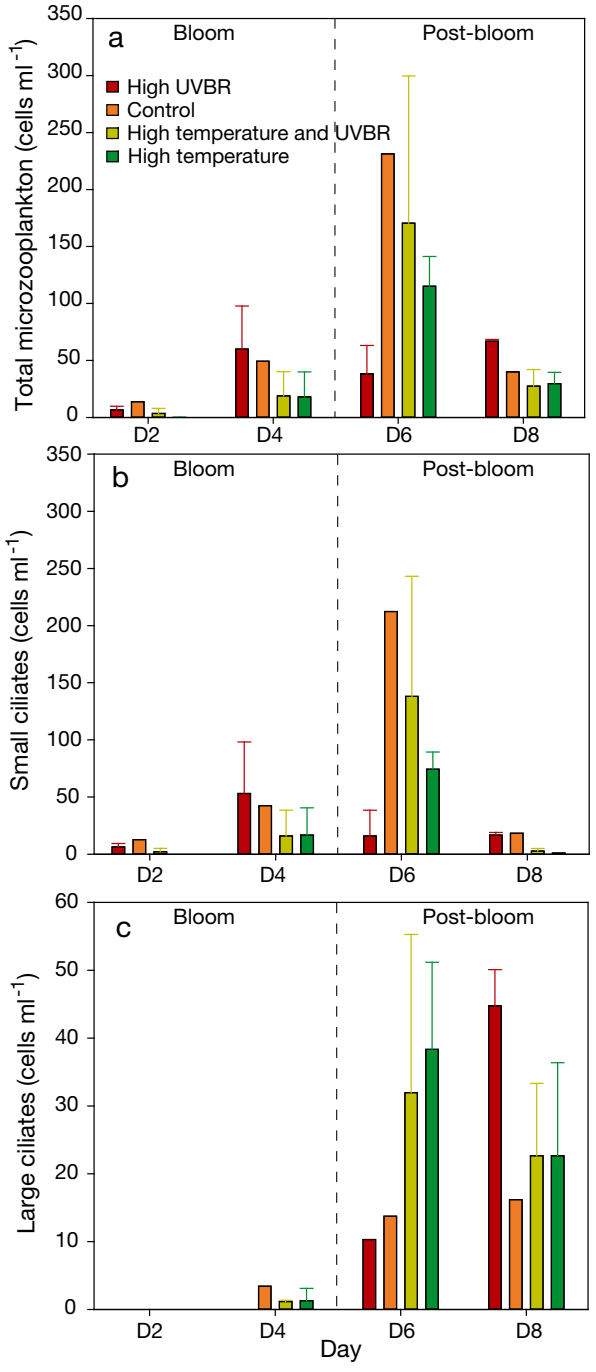

Fig. 8. Average (± SD) abundance of (a) total microzooplankton (cells ml^{-1}), (b) small ciliates (cells ml^{-1}), and (c) large ciliates (cells ml^{-1}) on Days 2, 4, 6, and 8 in the experimental mesocosms (see Fig. 2 for descriptions of the 4 treatment groups)

Day 8 in all treatments except in the high UVBR treatment (Fig. 8b). Except for Day 6, when small ciliates were significantly less abundant in the high UVBR treatment compared to the control ($p < 0.05$), there were no significant differences in total microzooplankton and small ciliate abundances among treatments.

In the high temperature treatments, the large ciliate abundance followed the same pattern (i.e. increasing from Day 2 to Day 6 before decreasing to Day 8, Fig. 8c). In contrast, the abundance of the large ciliates increased regularly from Day 2 to Day 8 in the control and the high UVBR treatment, although this increase was more pronounced in the high UVBR treatment than in the control. Finally, the abundance of the large ciliates presented an important difference between the normal and high temperature treatments on Day 6, although this difference was only significant between the high temperature and high UVBR treatments ($p < 0.05$).

DISCUSSION

It should be stressed that our results were obtained from a mesocosm experiment and cannot be fully, and without precautions, extrapolated to nature. Mesocosms are large outdoor enclosures, but scaling problems appear when trying to extrapolate results to the natural environment (Petersen et al. 2003). In addition, the increase in temperature that was applied in the present experiment is likely to occur on a much longer time scale (by ~2100) than in our study. In the course of global change, eurythermal organisms are likely to adapt to higher water temperatures, while stenothermal species should not tolerate these expected higher temperatures (Williamson et al. 2002). This should result in a modification of the composition and structure of marine ecosystems that cannot be predicted with our current state of knowledge. In contrast, the increase in UVBR that was used in the present study is already occurring due to the thinning of the stratospheric ozone layer (Casiccia et al. 2008) and will continue to be a threat to marine ecosystems until the ozone hole fully recovers towards 2070 (McKenzie et al. 2007). Despite these uncertainties, mesocosm experiments provide a valuable strategy for the understanding of short-term effects and to derive biological parameters that can be used to model future global change-induced modifications on marine ecosystems.

Temperature effects on the Beagle Channel microbial community

Temperature had a negative effect on total chl *a* (Fig. 3a) and on the abundance of the micro-sized diatom fraction (Fig. 5d) and bacteria (Fig. 7a) dur-

ing the post-bloom phase. In contrast, during the same period, temperature had a positive effect on the abundance of large nanophytoplankton (mainly prymnesiophytes, Fig. 5c). No effects of temperature were observed on the remainder of the plankton community. We discuss the possible reasons for the temperature effects observed on the plankton community.

The negative effects of temperature on the abundance of micro-sized diatoms did not appear to be caused by a cascading trophic effect, because the initial abundance of the most abundant mesozooplankton copepod (*Oithona similis*) observed in the mesocosms was only 3 ind. l^{-1} (G. Aguirre pers. comm.). This suggests that copepods did not control the biomass of micro-sized diatoms. In addition, it is probable that the growth of *O. similis* was not significant enough to influence its grazing impact through the duration of the experiment (Sabatini & Kiorboe 1994). Instead, we hypothesize that the differences observed between temperature treatments on micro-sized diatom abundance could have been caused by physiological responses. Temperature affects phytoplankton physiology and primary production via biochemical reactions (Cloern 1978). The decrease of micro-sized diatoms observed here contradicts the results of Montagnes & Franklin (2001), who showed that the growth rates of 8 diatom species responded linearly to an increase in temperature (between 9 and 25°C) and the observations of Lionard et al. (2012), who reported a positive effect of a 3°C temperature increase on the abundance of diatoms in the St. Lawrence Estuary. Conceivably, diatoms from southern Patagonia, which is a sub-polar ecosystem, are less likely adapted to, and do not benefit from, an increase in temperature.

Due to luxury uptake, diatoms do not necessarily assimilate all the nutrients they incorporate. Diatoms may accumulate nutrients within cells (e.g. vacuoles) and not use them readily (Dortch 1990, Bagwell 2009). Even though we observed no differences in nutrient concentrations between treatments, diatoms may have similar nutrient uptake rates between treatments but may have assimilated them at slower rates under warming conditions. Indeed, Lomas & Gilbert (2000), Berges et al. (2002), and Bagwell (2009) showed that the activity of the nitrate-reductase enzyme is lower for diatoms under high temperatures. Hence, the nitrate-reductase enzyme could be the key biological factor responsible for these observed differences in diatom biomass under different temperatures. Unfortunately, for our study, we do not have activity measurements that could support this hypothesis, so it should only be considered as a possible effect of temperature on phytoplankton.

This physiological effect may have benefited the large nanophytoplankton (here prymnesiophytes) in their competition for nutrients, and more particularly for nitrate (Brown et al. 2004). This hypothesis could also explain the higher biomass of the large nanophytoplankton observed in the high temperature compared to the normal temperature treatments during the post-bloom. Hare et al. (2007) also observed a shift in the phytoplankton community of the Bering Sea under warming, with the community being dominated by diatoms and nanophytoplankton in the low and high temperature treatments, respectively. They also attributed this change to a physiological effect of temperature on diatoms, possibly to the reduced activity of nitrate reductase under warming. Using *in situ* bottle incubation in the sub-Arctic Pacific, Noiri et al. (2005) also observed that diatoms were dominant at temperatures below 13°C and that nanophytoplankton was dominant at 18°C. They attributed these differences to different optimum temperatures of different phytoplankton groups and various metabolic functions. Using a large data set, Morán et al. (2010) also showed that the contribution of small phytoplankton cells (picophytoplankton) to the total phytoplankton biomass increases with temperature in the eastern and western North Atlantic Ocean. Finally, this result is also similar to the decrease in chl *a* observed under warming in the Arctic by Lara et al. (2013), and during which the abundance of large cells such as diatoms and dinoflagellates decreased with increasing temperature (A. Coello-Camba pers. comm.).

Elevated temperature also had a negative effect on bacterial abundance at the end of the experiment (i.e. on Days 8 and 9). A probable hypothesis for this effect is that the observed change in phytoplankton community composition altered the qualitative/quantitative composition of the dissolved organic matter (DOM) released, which may have been less suitable for the bacteria present within the mesocosms. For example, the chemical composition of diatom-derived DOM supports higher levels of bacterial richness, evenness, and phylogenetic diversity than DOM derived from cyanobacteria (Landa et al. 2013). Another hypothesis for the lower bacterial abundance under high temperature treatments could be related to the activity of heterotrophic flagellates <20 µm, which may have been important in this study. During a mesocosm experiment, Vidussi et al. (2011) and Fouilland et al. (2013) noticed a decrease in both the abundance and the production of bacteria

under warming conditions. They attributed this observation to a stronger grazing control by heterotrophic flagellates and ciliates. During the present experiment, the biomass and abundance of heterotrophic flagellates and small ciliates were not affected by temperature. Nevertheless, Vaqué et al. (2009) observed that bacterivorous grazing rates increased under warming conditions in Antarctica. Hence, it is possible that, despite the lack of differences in the biomass and abundance of heterotrophic flagellates and small ciliates observed under warming conditions, these organisms grazed more actively on bacteria.

UVBR effects on the Beagle Channel microbial community

Contrasting with the warming treatment, no overall UVBR effects on the Beagle Channel microbial community were observed during our experiment. The lack of a general UVBR effect on a planktonic microbial community studied under a mesocosm experiment goes against previously reported UVBR effects on the Beagle Channel community (Hernando et al. 2006, Longhi et al. 2006, Roy et al. 2006) and communities from other locations (e.g. Mostajir et al. 1999a,b, Chatila et al. 2001, Ferreyra et al. 2006). Other studies reported a more important effect of temperature than UVBR on planktonic communities (Vidussi et al. 2011, Fouilland et al. 2013). Below, we first reject some possible reasons why we did not observe UVBR effects on the planktonic community, i.e. weak UVBR intensities and higher photoprotective pigments concentrations. Then we discuss the possible reasons for this lack of an overall UVBR effect in the present study.

In this experiment, the shading effect at the surface of the mesocosms was very low, as the control mesocosms received 78 and 86% of the natural irradiance for 305 and 313 nm, respectively. Moreover, the addition of UVBR in the increased UVBR mesocosms was realistic and corresponded to a ~510% increase in UVBR relative to that received at the surface of the normal UVBR mesocosms. This is consistent with the results of radiation amplification factors given by Booth & Madronich (1994) for an ozone layer destruction of 60%. We compared the UVBR irradiance of the present study with other experiments where UVBR effects were observed (Longhi et al. 2006, Roy et al. 2006). The maximal natural UVBR irradiance (at 305 nm) measured at Ushuaia by Longhi et al. (2006) and Roy et al. (2006) was 3 µW cm^{-2} s^{-1}, whereas during the present study, the average natural irradiance at 305 nm was 2.67 ± 1.1 µW cm^{-2} s^{-1} (within 2 h before and after local noon). As for the present study, Longhi et al. (2006) and Roy et al. (2006) also simulated a 60% decrease in ozone layer thickness to study the effects of UVBR on the planktonic community. Therefore, UVBR irradiance used in the present study is comparable to that of the studies by Longhi et al. (2006) and Roy et al. (2006) and differences in UVBR cannot explain why there was no overall effect of UVBR on the planktonic community. Beagle Channel waters are characterized by a seasonal turbidity pattern, with clear waters in winter and more turbidity during summer (Venerus et al. 2005). Given the season of our experiment (summer), some UVBR could have been absorbed by the particles and the dissolved materials in the water column. However, the average depth of penetration of 1% of the UVBR in the present study (1.37 ± 0.07 m) is similar to the average depth of penetration of 1% of the UVBR (1.63 ± 0.72 m) reported by Longhi et al. (2006) for mesocosm studies that found significant UVBR effects on the planktonic communities in 3 locations at different latitudes: Rimouski (Canada), Ubatuba (Brazil), and Ushuaia (Argentina). Therefore, the attenuation of UVBR in the mesocosms cannot explain the lack of observed UVBR effects during our study. Hernando et al. (2002, 2011) found that the phytoplankton community produced photoprotective pigments such as mycosporine-like amino acids (MAAs) or antioxidants prior to their UVBR exposure experiments. This allowed the community to reduce the negative effects of UVBR. However, in the present experiment, no significant differences in MAA concentrations were observed between treatments (M. Hernando pers. obs.) and photoprotective pigments cannot explain the lack of UVBR effects on the planktonic community.

It is possible that the planktonic communities studied here were more resistant to UVBR due to the timing of the experiment (i.e. mid-austral summer, after the recovery of the ozone concentrations in the Southern Hemisphere). Compared to our study, the studies of Longhi et al. (2006) and Roy et al. (2006) were performed during the spring and, therefore, during the period of maximal exposure to the ozone hole. In addition, Helbling et al. (2001) observed lower UVBR effects when the phytoplankton community of Patagonia was composed of smaller cells, and Villafañe et al. (2004) observed lower photoinhibition of primary production in Patagonia before and after the phytoplankton bloom (2 periods dominated by small phytoplankton cells, i.e. pico- and nanophy-

toplankton) than during the bloom (dominated by larger phytoplankton cells, i.e. micro-sized diatoms). In this sense, intense micro-sized diatom blooms occur during austral spring (September–November) in the Beagle Channel, while assemblages dominated by small phytoflagellates are observed towards the end of austral summer (Almandoz et al. 2011). During this study, phytoplankton was dominated by pico- and nanophytoplankton in terms of abundance, which may explain the lack of observed UVBR effects on the phytoplankton.

Although no overall effect of UVBR was observed, some particular effects, or tendencies, were observed. The abundance of small ciliates was significantly lower in the enhanced UVBR treatment compared to the control on Day 6. Although the abundance of bacteria was lower under enhanced UVBR than in the control on Days 7, 8, and 9, differences were not significant. The small nanophytoplankton was significantly less abundant under enhanced UVBR than in the control at the end of the experiment (Days 6 to 9). These tendencies could indicate that if the experiment had lasted longer, UVBR might have had detectable effects on the plankton community and more particularly on its heterotrophic components. Indeed, several other studies (Mostajir et al. 1999b, Ferreyra et al. 2006, Vidussi et al. 2011, Llabrés et al. 2012) found that UVBR usually had a greater direct effect on heterotrophs than on autotrophic communities. In particular, because of their small volume and because some lack pigmentation, bacteria are considered among the most sensitive organisms to UVBR (Ruiz-González et al. 2013).

Finally, because we observed no overall UVBR effect on the microbial community, our results show that temperature and UVBR did not act synergistically or antagonistically in the present experiment. This is consistent with the study of Rae & Vincent (1998), who observed no synergistic effects of temperature and UVBR on subarctic freshwater communities. It is also consistent with the studies of Fouilland et al. (2013) and Vidussi et al. (2011), who observed significant effects of temperature on the abundance and the metabolic rates of the planktonic communities but no synergistic effects of temperature and UVBR. Finally, Lionard et al. (2012) also reported a greater effect of temperature than UVBR in structuring phytoplankton communities in the St. Lawrence Estuary. However, as discussed, if our experiment had lasted longer and UVBR effects had become detectable, synergistic or antagonistic effects of temperature and UVBR might have been observed.

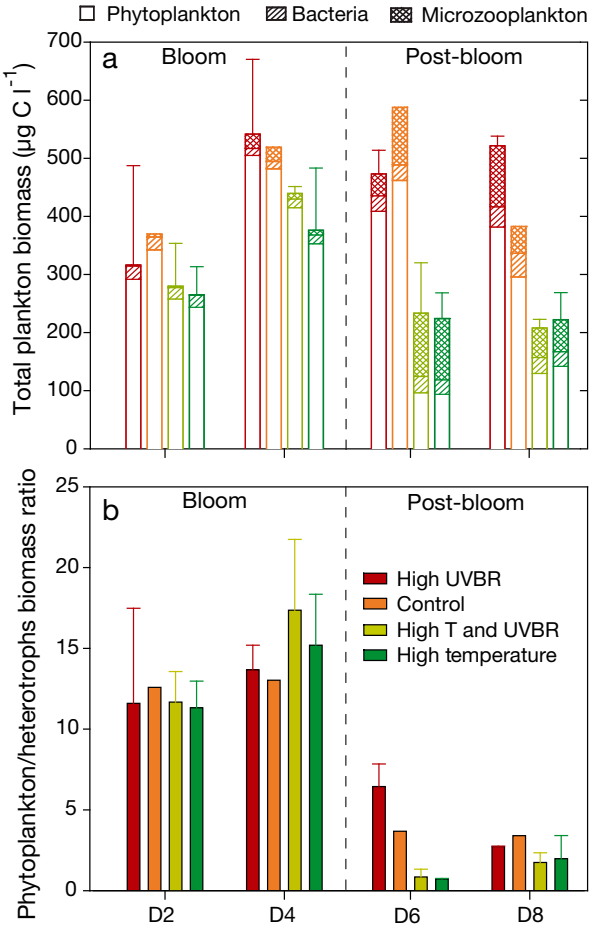

Fig. 9. (a) Average (± SD) of the total planktonic carbon biomass: phytoplankton, bacteria, and microzooplankton (µg C l^{-1}) on Days 2, 4, 6, and 8; and (b) average (± SD) of the ratio between total phytoplankton and heterotroph (bacteria + microzooplankton) biomasses in the experimental mesocosms (see Fig. 2 for descriptions of the 4 treatment groups)

Microbial food-web carbon dynamics

The total biomass of phytoplankton, bacterioplankton, and microzooplankton in carbon units is presented in Fig. 9a for Days 2, 4, 6, and 8 (i.e. days when simultaneous data were available) for the 4 treatments. The total plankton biomass was significantly lower ($p < 0.01$) in the high temperature treatments relative to the normal temperature treatments at the maximum of the bloom phase (Day 4) and during the post-bloom (Days 6 and 8). This lower biomass of the microbial community under the high temperature treatments was mainly due to the significantly lower phytoplankton carbon contribution, and particularly that of diatoms, observed in the high temperature treatments, as previously described. This is in agree-

ment with the results of Hare et al. (2007) who also observed an overall lower biomass of phytoplankton resulting from a shift in the community size structure from a dominance by diatoms under low temperature to a dominance by nanophytoplankton under warming. As previously stated, bacterial biomass was also significantly lower in these high temperature treatments during the post-bloom (Days 8 and 9, Fig. 7), but its impact on the total biomass of the microbial community was low. In addition, the biomass of total microzooplankton was not different between treatments, as previously mentioned.

Besides this overall lower biomass of the microbial community under elevated temperature, the system also evolved towards a more heterotrophic food web. Indeed, the ratio between the biomass of phytoplankton and the biomass of heterotrophs (bacteria and microzooplankton) was significantly lower in the elevated temperature treatments during the post bloom (i.e. on Days 6 and 8 although this was only significant on Day 6; $p < 0.05$, Fig. 9b). This implies that temperature had an overall effect on the structure of the community which may have implications for food-web dynamics and carbon cycling and settling. Consistent with our results, in 3 successive mesocosm experiments investigating the effects of temperature on pelagic food webs, Müren et al. (2005) observed that the autotroph:heterotroph biomass ratio decreased 5-fold when the temperature was raised from 5 to 10°C. In such a heterotrophic system, the respiration of the community would be higher than in the normal temperature treatments as observed by Müren et al. (2005). Lara et al. (2013) also observed that the activity and biomass of heterotrophs in the Arctic Ocean increased under warming, while the biomass of phototrophs decreased. Holding et al. (2013) suggested that the metabolism of planktonic communities in the Arctic switches from autotrophy to heterotrophy at a temperature threshold of 5°C. This was probably the case in the present experiment where the oxygen concentration and the fugacity of CO_2 (fCO_2) within the mesocosms were, respectively, lower and higher in the high temperature treatments (data not shown, X. Wang pers. comm.) although this was only significant for Days 2 and 6 for O_2 ($p < 0.05$) and Days 2, 4, 6, and 8 for fCO_2 ($p < 0.01$).

In addition, the total carbon biomass of the community in the elevated temperature treatments was lower at the end (Day 8) than at the beginning of the experiment (Day 2), which represents a loss of carbon from the system. We discuss below the possible fate of this carbon under elevated temperatures. First, this carbon could have been lost by bacterial respiration through microbial food-web interactions (exudation by phytoplankton, assimilation by bacteria and their respiration). As previously mentioned and as suggested by *in situ* O_2 and fCO_2 values, respiration was probably higher in the elevated temperature treatments compared to the normal temperature ones, and this is consistent with the carbon loss observed under warming. This carbon loss could also be linked to the transformation of POC into dissolved organic carbon (DOC; Mopper & Degens 1979). In fact, we observed that POC was significantly lower in the elevated temperature treatments during the post-bloom (Fig. 4). However, we do not have DOC values for the present study so we cannot confirm this hypothesis. Another possibility would be that this carbon was transferred via predation of bacteria to the smaller heterotrophic flagellate size fraction, which, as previously mentioned, may have been under-estimated in the present study. Finally, this carbon may have sedimented to the bottom of the mesocosms in the form of dead cells or aggregated particulate matter and feces. Although we did not measure sedimentation, it is unlikely that sedimentation was higher under elevated temperature since Müren et al. (2005) observed a decrease in the organic carbon sedimentation when temperature was elevated from 5 to 10°C probably because of the increased respiration losses and the biodegradation of organic carbon by bacteria.

Finally, most of the treatment effects that occurred in the present experiment were observed during the post-bloom. This is a common result of mesocosm experiments. For example, Mostajir et al. (1999a) observed that the abundances of nanophytoplankton and ciliates (15–35 µm) decreased by 63 and 66% under the effect of UVBR. Due to the decrease in predation, the abundances of smaller cells increased (by 50, 40, and 300% for bacteria, picophytoplankton, and heterotrophic flagellates, respectively). Ferreyra et al. (2006) observed a similar cascading trophic effect in another mesocosm experiment. In both of these experiments, the effects of UVBR were observed towards the end of the experiment, during the stationary phase or the post bloom. Vidussi et al. (2011) observed significant shifts in the plankton, food-web structure and function under warming in Mediterranean coastal waters. Working on the same mesocosm experiment, both a decrease in bacterial production and an increase in primary production under warming were reported by Fouilland et al. (2013). In these 2 studies, the effects of temperature became significant midway through the experiment.

In a review of 10 mesocosm experiments on the effects of UVBR on plankton organisms, Belzile et al. (2006) underlined that bloom conditions are generally observed in mesocosm experiments, with chl *a* increasing up to 25-fold. However, they noticed that the bloom lasted only a few days when no nutrients were added. Therefore, adding nutrients probably delayed the response of the planktonic community to the treatments in the present and in other mesocosm experiments. In fact, we believe that the effects of nutrient enrichment can be so strong that the effects of other forcing factors (e.g. UVBR) are hidden during the bloom. This may explain why no response of the planktonic community was detected during the bloom and why the few UVBR effects and the strong temperature effects that were observed in the present study occurred towards the end of the experiment.

CONCLUSION

Because no major UVBR effects were observed, whereas warming had a profound effect on the microbial community, our results show that these 2 stressors did not act synergistically or antagonistically in the present experiment. The lack of a major UVBR effect might be related to the timing of the experiment (i.e. mid-austral summer, after the recovery of the ozone concentrations in the Southern Hemisphere). In this sense, the planktonic communities present at that time might have been already adapted/resistant to UVBR. In addition, UVBR effects might have become detectable if the experiment had lasted longer. In contrast, temperature had an overall impact on the total biomass and the structure of the microbial community, favoring the lower trophic levels such as nanophytoplankton (mainly prymnesiophytes here) and bacteria. Although the reasons for these impacts of temperature on the components of the microbial community remain hypothetical, they might have implications on whole food-web dynamics and carbon cycling. For example, a modification of the structure and/or composition of the microbial community towards a microbial food web composed of small cells may have consequences on carbon fluxes within the marine food web (Legendre & Rivkin 2002) and on the fate of carbon within the water column (e.g. carbon sedimentation to the deep ocean layers, Legendre & Rassoulzadegan 1996). Our results provide new evidence for a clear impact of increasing temperature on the planktonic food web for the sub-Antarctic region.

Acknowledgements. This research is part of the project 'Combined Effects of Ultraviolet-B Radiation, Increased CO2 and Climate Warming on the Biological Pump: a Temporal and Latitudinal Study', led by S.D. and supported by the Natural Sciences and Engineering Research Council of Canada (NSERC, SRO Grant# 334876-2005), and by a grant from the Instituto Antártico Argentino (IAA) to G.A.F. in the frame of the project 'Research on Ultraviolet and Global warming effects on Biological pump Yields' (RUGBY). We thank Pascal Rioux and Prof. Émilien Pelletier for providing the data for nutrients and POC-PON. We also gratefully thank Dr. Mariano Mémolli, director of the Dirección Nacional del Antártico, as well as the authorities of the Centro de Investigaciones Australes (CADIC) from Ushuaia, particularly G. Lovrich, and the numerous people from ISMER and IAA who helped us with the set-up of the mesocosms and the experiment in Ushuaia, including Sylvain Leblanc, Patrick Poulin, Alejandro Olariaga, Alejandro Ulrich, Eugenia di Fiori and Raúl Codina. This work is a contribution to the Institut des sciences de la mer de Rimouski (ISMER), the Université catholique de Louvain and to IAA. S.M. is a postdoctoral researcher with the Fond de la Recherche de Scientifique.

LITERATURE CITED

Almandoz GO, Hernando MP, Ferreyra GA, Schloss IR, Ferrario ME (2011) Seasonal phytoplankton dynamics in extreme southern South America (Beagle Channel, Argentina). J Sea Res 66:47–57

Bagwell JE (2009) Transcriptional response of nitrogen uptake and assimilation in marine diatoms; *Thalassiosira pseudonana* and *Thalassiosira weissflogii*. MSc, University of North Carolina Wilmington, Wilmington, NC

Belzile C, Demers S, Ferreyra GA, Schloss I and others (2006) UV effects on marine planktonic food webs: a synthesis of results from mesocosm studies. Photochem Photobiol 82:850–856

Berges JA, Varela DE, Harrison PJ (2002) Effects of temperature on growth rate, cell composition and nitrogen metabolism in the marine diatom *Thalassiosira pseudonana* (Bacillariophyceae). Mar Ecol Prog Ser 225:139–146

Booth CR, Madronich S (1994) Radiation amplification factors: improved formulation accounts for large increases in ultraviolet radiation associated with Antarctic ozone depletion. Antarct Res Ser 62:39–43

Børsheim KY, Bratbak G (1987) Cell volume to cell carbon conversion factors for a bacterivorous *Monas* sp. enriched from seawater. Mar Ecol Prog Ser 36:171–175

Bouchard JN, Roy S, Campbell DA (2006) UVB Effects on the photosystem II-D1 protein of phytoplankton and natural phytoplankton communities. Photochem Photobiol 82:936–951

Brown JH, Gillooly JF, Allen AP, Savage VM, West GB (2004) Toward a metabolic theory of ecology. Ecology 85: 1771–1789

Casiccia C, Zamorano F, Hernandez A (2008) Erythemal irradiance at the Magellan's region and Antarctic ozone hole 1999-2005. Atmosfera 21:1–12

Chatila K, Demers S, Mostajir B, Gosselin M, Chanut JP, Monfort P, Bird D (2001) The responses of a natural bacterioplankton community to different levels of ultraviolet-B radiation: a food web perspective. Microb Ecol 41:56–68

Christensen JH, Hewitson B, Busuioc A, Chen A and others (2007) Regional climate projections. In: Solomon S, Qin D, Manning M, Chen Z and others (eds) Climate Change 2007: the physical science basis. Contribution of Working Group I to the Fourth Assessment Report of the Intergovernmental Panel on Climate Change. Cambridge University Press, Cambridge, p 847–940

Cloern JE (1978) Empirical model of *Skeletonema costatum* photosynthetic rate, with applications in the San Francisco Bay estuary. Adv Water Resour 1:267–274

Díaz S, Carnilion C, Escobar J, Deferrari G and others (2006) Simulation of ozone depletion using ambient irradiance supplemented with UV lamps. Photochem Photobiol 82: 857–864

Dortch Q (1990) The interaction between ammonium and nitrate uptake in phytoplankton. Mar Ecol Prog Ser 61: 183–201

Ferreyra GA, Mostajir B, Schloss IR, Chatila K and others (2006) Ultraviolet-B radiation effects on the structure and function of lower trophic levels of the marine planktonic food web. Photochem Photobiol 82:887–897

Fouilland E, Mostajir B, Torréton JP, Bouvy M and others (2013) Microbial carbon and nitrogen production under experimental conditions combining warming with increased ultraviolet-B radiation in Mediterranean coastal waters. J Exp Mar Biol Ecol 439:47–53

Gasol JM, Giorgio PAD (2000) Using flow cytometry for counting natural planktonic bacteria and understanding the structure of planktonic bacterial communities. Sci Mar 64:197–224

Gasol JM, Zweifel UL, Peters F, Fuhrman JA, Hagström Å (1999) Significance of size and nucleic acid content heterogeneity as measured by flow cytometry in natural planktonic bacteria. Appl Environ Microbiol 65: 4475–4483

Giordanino MVF, Strauch SM, Villafañe VE, Helbling EW (2011) Influence of temperature and UVR on photosynthesis and morphology of four species of cyanobacteria. J Photochem Photobiol B 103:68–77

Grasshoff K, Ehrhardt M, Kremling K (1983) Methods of seawater analysis. Verlag Chemie, Weinheim

Häder DP, Sinha RP (2005) Solar ultraviolet radiation-induced DNA damage in aquatic organisms: potential environmental impact. Mutat Res 571:221–233

Häder DP, Kumar HD, Smith RC, Worrest RC (2007) Effects of solar UV radiation on aquatic ecosystems and interactions with climate change. Photochem Photobiol Sci 6: 267–285

Halac SR, Villafañe VE, Helbling EW (2010) Temperature benefits the photosynthetic performance of the diatoms *Chaetoceros gracilis* and *Thalassiosira weissflogii* when exposed to UVR. J Photochem Photobiol B 101:196–205

Hare CE, Leblanc K, DiTullio GR, Kudela RM and others (2007) Consequences of increased temperature and CO_2 for phytoplankton community structure in the Bering Sea. Mar Ecol Prog Ser 352:9–16

Helbling EW, Buma AGJ, de Boer MK, Villafañe VE (2001) *In situ* impact of solar ultraviolet radiation on photosynthesis and DNA in temperate marine phytoplankton. Mar Ecol Prog Ser 211:43–49

Hernando M, Carreto JI, Carignan MO, Ferreyra GA, Gross C (2002) Effects of solar radiation on growth and mycosporine-like amino acids content in *Thalassiosira* sp, an Antarctic diatom. Polar Biol 25:12–20

Hernando M, Schloss I, Roy S, Ferreyra G (2006) Photoacclimation to long-term ultraviolet radiation exposure of natural sub-Antarctic phytoplankton communities: fixed surface incubations versus mixed mesocosms. Photochem Photobiol 82:923–935

Hernando M, Malanga G, Puntarulo S, Ferreyra G (2011) Non-enzymatic antioxidant photoprotection against potential UVBR-induced damage in an Antarctic diatom (*Thalassiosira* sp.). Lat Am J Aquat Res 39:397–408

Hillebrand H, Dürselen CD, Kirschtel D, Pollingher U, Zohary T (1999) Biovolume calculation for pelagic and benthic microalgae. J Phycol 35:403–424

Holding JM, Duarte CM, Arrieta JM, Vaquer-Suyner R, Coello-Camba A, Wassmann P, Agustí S (2013) Experimentally determined temperature thresholds for Arctic plankton community metabolism. Biogeosciences 10: 357–370

Houghton JT, Ding Y, Griggs DJ, Noguer M and others (2001) Climate Change 2001: the scientific basis. Contribution of Working Group I to the Third Assessment Report of the Intergovernmental Panel on Climate Change. Cambridge University Press, Cambridge

Ingram RG (1979) Symposium on the oceanography of the St. Lawrence Estuary. Water mass modification in the St. Lawrence Estuary. Nat Can 106:45–54

Jeffrey SW, Wright SW (2006) Photosynthetic pigments in marine microalgae: insights from cultures and the sea. In: Subba Rao DV (ed) Algal cultures, analogues of blooms and applications, Book 1. Science Publishers, Enfield, NH, p 33–90

Kirk JTO (1994) Light and photosynthesis in aquatic systems. Cambridge University Press, Cambridge

Landa M, Cottrell MT, Kirchman DL, Kaiser K and others (2013) Phylogenetic and structural response of heterotrophic bacteria to dissolved organic matter of different chemical composition in a continuous culture study. Environ Microbiol, doi:10.1111/1462-2920.12242

Lara E, Arrieta JM, Garcia-Zarandona I, Boras JA and others (2013) Experimental evaluation of the warming effect on viral, bacterial and protistan communities in two contrasting Arctic systems. Aquat Microb Ecol 70:17–32

Lebaron P, Servais P, Agogue H, Courties C, Joux F (2001) Does the high nucleic acid content of individual bacterial cells allow us to discriminate between active cells and inactive cells in aquatic systems? Appl Environ Microbiol 67:1775–1782

Legendre L, Rassoulzadegan F (1995) Plankton and nutrient dynamics in marine waters. Ophelia 41:153–172

Legendre L, Rassoulzadegan F (1996) Food-web mediated export of biogenic carbon in oceans: hydrodynamic control. Mar Ecol Prog Ser 145:179–193

Legendre L, Rivkin RB (2002) Pelagic food webs: responses to environmental processes and effects on the environment. Ecol Res 17:143–149

Li WKW, McLaughlin FA, Lovejoy C, Carmack EC (2009) Smallest algae thrive as the Arctic Ocean freshens. Science 326:539

Lionard M, Roy S, Tremblay-Létourneau M, Ferreyra GA (2012) Combined effects of increased UV-B and temperature on the pigment-determined marine phytoplankton community of the St. Lawrence Estuary. Mar Ecol Prog Ser 445:219–234

Llabrés M, Agustí S, Fernández M, Canepa A, Maurin F, Vidal F, Duarte CM (2012) Impact of elevated UVB radiation on marine biota: a meta-analysis. Glob Ecol Biogeogr 22:131–144

Lomas MW, Gilbert PM (2000) Comparisons of nitrate uptake, storage, and reduction in marine diatoms and flagellates. J Phycol 36:903–913

Longhi ML, Ferreyra G, Schloss I, Roy S (2006) Variable phytoplankton response to enhanced UV-B and nitrate addition in mesocosm experiments at three latitudes (Canada, Brazil and Argentina). Mar Ecol Prog Ser 313: 57–72

Mackey MD, Mackey DJ, Higgins HW, Wright SW (1996) CHEMTAX - a program for estimating class abundances from chemical markers: application to HPLC measurements of phytoplankton. Mar Ecol Prog Ser 144:265–283

Manney GL, Santee ML, Rex M, Livesey NJ and others (2011) Unprecedented Arctic ozone loss in 2011. Nature 478:469–475

McKenzie RL, Aucamp PJ, Bais AF, Björnd LO, Ilyas M (2007) Changes in biologically-active ultraviolet radiation reaching the Earth's surface. Photochem Photobiol Sci 6:218–231

Menden-Deuer S, Lessard EJ (2000) Carbon to volume relationships for dinoflagellates, diatoms, and other protist plankton. Limnol Oceanogr 45:569–579

Montagnes DJS, Franklin DJ (2001) Effect of temperature on diatom volume, growth rate, and carbon and nitrogen content: reconsidering some paradigms. Limnol Oceanogr 46:2008–2018

Montagnes DJS, Berges JA, Harrison PJ, Taylor FJR (1994) Estimating carbon, nitrogen, protein, and chlorophyll *a* from volume in marine phytoplankton. Limnol Oceanogr 39:1044–1060

Montes-Hugo M, Doney SC, Ducklow HW, Fraser W, Martinson D, Stammerjohn SE, Schofield O (2009) Recent changes in phytoplankton communities associated with rapid regional climate change along the western Antarctic Peninsula. Science 323:1470–1473

Mopper K, Degens ET (1979) Organic carbon in the ocean: nature and cycling. In: Bolin B, Degens ET, Kempe S, Ketner P (eds) The global carbon cycle. John Wiley & Sons, p 293–316

Morán XAG, López-Urrutia T, Calvo-Díaz A, Li WKW (2010) Increasing importance of small phytoplankton in a warmer ocean. Glob Change Biol 16:1137–1144

Moreau S, Ferreyra GA, Mercier B, Lemarchand K and others (2010) Variability of the microbial community in the Western Antarctic Peninsula from late fall to spring during a low-ice cover year. Polar Biol 33:1599–1614

Moreau S, Schloss IR, Mostajir B, Demers S, Almandoz GO, Ferrario ME, Ferreyra GA (2012) Influence of microbial community composition and metabolism on air–sea ΔpCO_2 variation off the western Antarctic Peninsula. Mar Ecol Prog Ser 446:45–59

Moreau S, di Fiori E, Schloss IR, Almandoz GO, Esteves JL, Paparazzo FE, Ferreyra GA (2013) The role of phytoplankton composition and microbial community metabolism in sea–air ΔpCO2 variation in the Weddell Sea. Deep-Sea Res I 82:44–59

Mostajir B, Demers S, De Mora S, Belzile C and others (1999a) Experimental test of the effect of ultraviolet-B radiation in a planktonic community. Limnol Oceanogr 44:586–596

Mostajir B, Sime-Ngando T, Demers S, Belzile C and others (1999b) Ecological implications of changes in cell size and photosynthetic capacity of marine Prymnesiophyceae induced by ultraviolet-B radiation. Mar Ecol Prog Ser 187:89–100

Müren U, Berglund J, Samuelsson K, Andersson A (2005) Potential effects of elevated sea-water temperature on pelagic food webs. Hydrobiologia 545:153–166

Neale PJ, Helbling EW, Zagarese HE (2003) Modulation of UVR exposure and effects by vertical mixing and advection. In: Helbling EW, Zagarese H (eds) UV Effects in aquatic organisms and ecosystems. The Royal Society of Chemistry, Cambridge, p 107–134

Noiri Y, Kudo I, Kiyosawa H, Nishioka J, Tsuda A (2005) Influence of iron and temperature on growth, nutrient utilization ratios and phytoplankton species composition in the western subarctic Pacific Ocean during the SEEDS experiment. Prog Oceanogr 64:149–166

Orce VL, Helbling EW (1997) Latitudinal UVR-PAR measurements in Argentina: extent of the 'ozone hole'. Global Planet Change 15:113–121

Petersen JE, Kemp WM, Bartleson R, Boynton WR and others (2003) Multiscale experiments in coastal ecology: improving realism and advancing theory. BioScience 53: 1181–1197

Putt M, Stoecker DK (1989) An experimentally determined carbon:volume ratio for marine 'oligotrichous' ciliates from estuarine and coastal waters. Limnol Oceanogr 34: 1097–1103

Rae R, Vincent WF (1998) Effects of temperature and ultraviolet radiation on microbial foodweb structure: potential responses to global change. Freshw Biol 40: 747–758

Roy S, Mohovic B, Gianesella SMF, Schloss I, Ferrario M, Demers S (2006) Effects of enhanced UV-B on pigment-based phytoplankton biomass and composition of mesocosm-enclosed natural marine communities from three latitudes. Photochem Photobiol 82:909–922

Ruiz-González C, Simó R, Sommaruga R, Gasol JM (2013) Away from darkness: a review on the effects of solar radiation on heterotrophic bacterioplankton activity. Front Microbiol, doi: 10.3389/fmicb.2013.00131

Sabatini M, Kiorboe T (1994) Egg production, growth and development of the cyclopoid copepod *Oithona similis*. J Plankton Res 16:1329–1351

Sarmiento JL, Slater R, Barber R, Bopp L and others (2004) Response of ocean ecosystems to climate warming. Global Biogeochem Cycles 18, GB3003, doi:10.1029/2003GB002134

Schloss IR, Ferreyra GA, Ferrario ME, Almandoz GO and others (2007) Role of plankton communities in sea–air variations in pCO_2 in the SW Atlantic Ocean. Mar Ecol Prog Ser 332:93–106

Sinha RP, Häder DP (2002) UV-induced DNA damage and repair: a review. Photochem Photobiol Sci 1:225–236

Tarran GA, Heywood JL, Zubkov MV (2006) Latitudinal changes in the standing stocks of nano- and picoeukaryotic phytoplankton in the Atlantic Ocean. Deep-Sea Res II 53:1516–1529

Thompson DWJ, Solomon S (2002) Interpretation of recent southern hemisphere climate change. Science 296: 895–899

Thyssen M, Ferreyra G, Moreau S, Schloss I, Denis M, Demers S (2011) The combined effect of ultraviolet B radiation and temperature increase on phytoplankton dynamics and cell cycle using pulse shape recording flow cytometry. J Exp Mar Biol Ecol 406:95–107

Utermöhl H (1958) Zur Vervollkommnung der quantitativen Phytoplankton-Methodik. Mitt Int Ver Theor Angew Limnol 9:1–38

Vaqué D, Casamayor EO, Gasol JM (2001) Dynamics of whole community bacterial production and grazing losses in seawater incubations as related to the changes in the proportions of bacteria with different DNA content. Aquat Microb Ecol 25:163–177

Vaqué D, Guadayol Ò, Peters F, Felipe J, Malits A, Pedrós-Alió C (2009) Differential response of grazing and bacterial heterotrophic production to experimental warming in Antarctic waters. Aquat Microb Ecol 54: 101–112

Vasseur C, Mostajir B, Nozais C, Denis M, Fouilland É, Klein B, Demers S (2003) Effects of bio-optical factors on the attenuation of ultraviolet and photosynthetically available radiation in the North Water Polynya, northern Baffin Bay: ecological implications. Mar Ecol Prog Ser 252: 1–13

Venerus L, Calcagno J, Lovrich G, Nahabedian D (2005) Differential growth of the barnacle *Notobalanus flosculus* (Archaeobalanidae) onto artificial and live substrates in the Beagle Channel, Argentina. Helgol Mar Res 59: 196–205

Vidussi F, Mostajir B, Fouilland E, Le Floc'h E and others (2011) Effects of experimental warming and increased ultraviolet B radiation on the Mediterranean plankton food web. Limnol Oceanogr 56:206–218

Villafañe VE, Barbieri ES, Helbling EW (2004) Annual patterns of ultraviolet radiation effects on temperate marine phytoplankton off Patagonia, Argentina. J Plankton Res 26:167–174

Williamson CE, Grad G, De Lange HJ, Gilroy S, Karapelou DM (2002) Temperature dependent ultraviolet responses in zooplankton: implications of climate change. Limnol Oceanogr 47:1844–1848

Zapata M, Rodríguez F, Garrido JL (2000) Separation of chlorophylls and carotenoids from marine phytoplankton: a new HPLC method using a reversed phase C_8 column and pyridine-containing mobile phases. Mar Ecol Prog Ser 195:29–45

Zubkov MV, Sleigh MA, Burkill PH (2000a) Assaying picoplankton distribution by flow cytometry of underway samples collected along a meridional transect across the Atlantic Ocean. Aquat Microb Ecol 21:13–20

Zubkov MV, Sleigh MA, Burkill PH, Leakey RJG (2000b) Picoplankton community structure on the Atlantic Meridional Transect: a comparison between seasons. Prog Oceanogr 45:369–386

Editorial responsibility: Ruben Sommaruga, Innsbruck, Austria

Submitted: October 10, 2013; Accepted: March 12, 2014
Proofs received from author(s): April 25, 2014